Chemosphere 210 (2018) 215–223

Contents lists available at ScienceDirect

Chemosphere

journal homepage: www.elsevier.com/locate/chemosphere

Molecular understanding of the interaction of amino acids with sulfuric acid in the presence of water and the atmospheric implication

Pu Ge [a], Gen Luo [a], Yi Luo [a, *], Wei Huang [b], Hongbin Xie [c], Jingwen Chen [c], Jingping Qu [a]

[a] State Key Laboratory of Fine Chemicals, School of Chemical Engineering, Dalian University of Technology, Dalian, 116024, China
[b] School of Environmental Science & Optoelectronic Technology, University of Science and Technology of China, Hefei, Anhui, 230026, China
[c] Key Laboratory of Industrial Ecology and Environmental Engineering (MOE), School of Environmental Science and Technology, Dalian University of Technology, Dalian, 116024, China

HIGHLIGHTS

- Structural differences of amino acids have great influence on cluster structures.
- (Thr) (SA) clusters may participate in ion-induced nucleation.
- Serine may play more important role in stabilizing sulfuric acid.
- Hydrated (Ser) (SA) and (Tur) (SA) clusters could retain water even at low RH.
- Amino acid clusters possess stronger Rayleigh light scattering intensities.

GRAPHICAL ABSTRACT

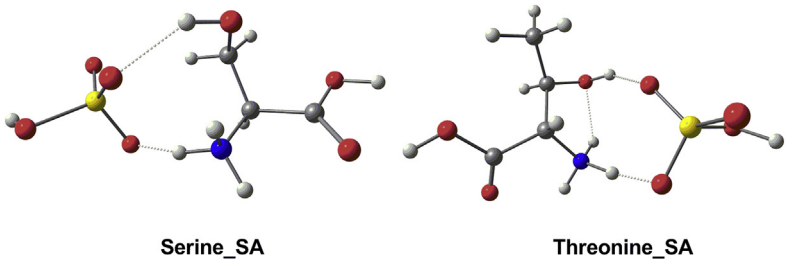

ARTICLE INFO

Article history:
Received 30 April 2018
Received in revised form
29 June 2018
Accepted 2 July 2018
Available online 4 July 2018

Handling Editor: R. Ebinghaus

Keywords:
Serine
Threonine
GRRM
New particle formation
Hydroxyl group
Methyl substitution

ABSTRACT

Amino acids are important components of atmospheric aerosols. Despite the diversity of amino acids structures, however, the role of amino acids with additional non-characteristic functional groups in new particle formation (NPF) has almost remained unexplored. Herein, the interaction of serine (Ser) and threonine (Thr), which feature a hydroxyl group and differ by a methyl-substitution, with sulfuric acid (SA) and up to three water (W) molecules has been investigated at the M06-2X/6-311++G (3df, 3pd) level of theory. The effects of structural differences of amino acids on the structure and properties of clusters were also pointed out. Results show that serine may play more important role in stabilizing sulfuric acid to promote NPF in initial steps compared with threonine, glycine and alanine. Meanwhile, threonine may participate in ion-induced nucleation due to the high dipole moment of (Thr) (SA) isomers. Moreover, the effects of structure differences of amino acids can be seen in several aspects. Firstly, methyl substitution and hydroxyl group of amino acids have great influence on the structure of clusters. Secondly, hydrated (Ser) (SA) and (Tur) (SA) clusters could retain water even at low relative humidity, which may due to the hydroxyl group in serine and threonine. In addition, the Rayleigh light scattering intensities of amino acid-containing clusters are higher than trimethylamine, monoethanolamine and oxalic acid-involved counterparts. The effect of carboxyl group and methyl substitution on optical properties of clusters is also discussed. This study may bring new insight into the role of amino acids with additional non-characteristic functional groups in initial steps of NPF.

* Corresponding author.
E-mail address: luoyi@dlut.edu.cn (Y. Luo).

https://doi.org/10.1016/j.chemosphere.2018.07.014
0045-6535/

1. Introduction

Aerosols have received much attention as they can significantly influence climate (Baker and Peter, 2008) and human health (Dimitriou and Kassomenos, 2017; Saikia et al., 2016). New particle formation (NPF) is one of the primary sources of atmospheric aerosol particles, (Merikanto et al., 2009) which includes the formation of stabilized clusters through nucleation and subsequent growth (Zhang et al., 2011). However, the underlying mechanism of NPF remains poorly understood, especially for its initial steps. The composition and population of clusters in the initial nucleation is crucial and they would affect the nucleation rate and the NPF events. Sulfuric acid (SA) is a primary driver of atmospheric particle nucleation (Lyu et al., 2018; Kulmala et al., 2006). The participation of organics such as amines, (Nadykto et al., 2015) organic acids, (Zhang et al., 2004) aldehydes, (Shi et al., 2018) and highly oxidized multifunctional organic molecules (HOMs) (Li et al., 2017) acting as stabilizing compounds in nucleation has been proposed. It turns out that the interaction of organics with SA is an important step in nucleation (Metzger et al., 2010). In Xie's work, the interaction of monoethanolamine (MEA) and SA was proposed to be rate-determining step in nucleation (Xie et al., 2017).

Water-soluble organic nitrogen compounds constitute a major portion of fine aerosol particles (Zhang et al., 2002; Choi et al., 2015; Barbaro et al., 2017; Paula et al., 2016). Free amino acids make up a considerable portion of particulate organic nitrogen (Ge et al., 2011; Matos et al., 2016; Scalabrin et al., 2012). Besides, alanine has been detected in urban air adjacent to a municipal incinerator, waste collection center and sewage treatment plant (Leach et al., 1999). Considering their atmospheric abundance, amino compounds are likely to participate in NPF and affect the property of aerosols. However, the studies of the role of amino acids as potential nucleation stabilizer and their effect on aerosols are limited. Elm et al. (2013) found that glycine in all three protonation states is found to have a favorable interaction with SA, higher than that of ammonia. Besides, the deprotonated glycine molecule is found to yield the highest stabilizing effect on the sulfuric acid clusters through the interaction of both the amino and carboxylic moieties, while the protonated glycine molecule is found to have a high stabilizing effect on the addition of water and ammonia. Huang et al. (Wang et al., 2016) pointed out that alanine can interact with H_2SO_4 and H_2O by both amino group and carbonyl group, and that it has a higher cluster stabilizing effect than that of ammonia. Huang et al. (Wang et al., 2016) also indicated that a higher humidity and temperature could contribute to the formation of hydrated clusters of alanine. However, to the best of our knowledge, the role of amino acids with additional non-characteristic functional groups in NPF has almost remained unexplored.

Previous studies have indicated that the number and location of functional groups have influence on the viscosity and cloud condensation nucleus (CCN) efficiency of organic aerosol (Suda et al., 2014; Rothfuss and Petters, 2016). The effects of different functional groups of organics on the structure of clusters and stabilizing abilities of organic-sulfuric acid clusters have been studied (Elm et al., 2017). Particularly, the role of hydroxyl group in enhancing nucleation ability of monoethanolamine (MEA) is addressed (Xie et al., 2017). Amino acids are various with different additional non-characteristic functional groups. Serine and threonine, possessing a hydroxyl group compared with glycine and alanine (Fig. 1), are detected to be abundant free amino acids in atmospheric aerosols (Barbaro et al., 2011). Studies indicated that free amino acids in $PM_{2.5}$ were enriched in protein-type amino species such as glycine, threonine, serine and alanine (Zhang and Anastasio, 2003). Besides, previous studies also showed that organics with different methyl-substitutions, such as methylamine and trimethylamine (TMA), perform differently in nucleation (Arquero et al., 2017a, 2017b). Therefore, serine and threonine, which feature a hydroxyl group and differ by a methyl-substitution, may have distinct effects on the initial steps of NPF. In this study, the interaction of SA with two amino acids, threonine (Thr) and serine (Ser), has been computationally studied. Hydration effect was considered with up to three water (W) molecules, as the effect of the forth water may be minimal (Xie et al., 2017). Hydrate distributions and Rayleigh light scattering intensities of (Ser) (SA) $(W)_n$ $(n = 0–3)$ and (Thr) (SA) $(W)_n$ $(n = 0–3)$ clusters were investigated. Besides, the effects of structural differences such as hydroxyl group or methyl substitution of amino acids on the structures and properties of clusters were also addressed.

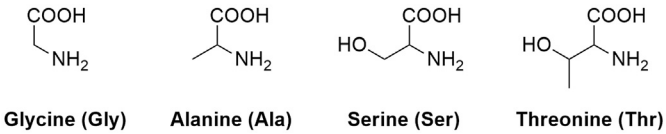

Glycine (Gly) Alanine (Ala) Serine (Ser) Threonine (Thr)

Fig. 1. The structures of glycine, alanine, serine, and threonine. The abbreviations of the four amino acids are shown in parentheses.

2. Computational details

In this study, the GRRM program (version 14) was used in combination with the Gaussian 09 (Frisch et al., 2016) program package to search for the global minima of (Ser) (SA) $(W)_n$ $(n = 0–3)$ and (Thr) (SA) $(W)_n$ $(n = 0–3)$ clusters. The scaled hypersphere search (SHS) method, which is an uphill-walking technique, was utilized to automatically explore the reaction pathway from a given equilibrium structure (EQ) (Maeda and Ohno, 2005; Ohno and Maeda, 2004, 2006). Such an exploration of reaction pathways is executed by detecting and following anharmonic downward distortions (ADDs) (Maeda and Ohno, 2008). This ADD following is a new concept based on a kind of principle that has arisen from deep considerations on the feature of potential energy surface (PES). To effectively detect the ADD, a given EQ-centered hypersphere surface is introduced in the SHS technique. During the reaction pathway following on the scaled hypersphere surface, the conventional optimization scheme and downhill-walking technique may be utilized. By detecting and following all of the ADDs for a given EQ, the SHS method can find transition states, dissociation channels, and other EQs. Such detection and following are automatically done for each newly found EQ via a one-after-another manner. Since the occurrence of a chemical reaction shows an ADD as a symptom and the lowest-energy minimum should not be out of connection with other EQs on the global potential energy surface, we believe that most of the important EQs at the low-energy region should be found by the SHS method. After the reaction pathways are traced for all the obtained EQs, the global potential energy surface may be figured. As shown in the applications to $(H_2O)_8$ and $H^+(H_2O)_8$, the search for known important structures as well as global potential energy minimum of H-bond clusters has been achieved (Maeda and Ohno, 2007; Luo et al., 2007). Specifically, molecular energy and its gradient (Hessian matrix) were calculated at the HF/6-31G level. The HF/6-31G level of method was chosen for efficiency of exploration (Lin et al., 2014). For the efficiency of the exploration, we imposed the following conditions (Omori et al., 2014) on GRRM calculations: (1) start with 24 randomly created conformations; (2) to accelerate pathway exploration via ADD, the largest ADD technique was applied by setting the parameter LADD to be 5; (3) optimize the structure only for EQs and skip the optimization of the transition structures.

As over 1000 isomers are obtained for each cluster, only the isomers within 6–7 kcal/mol of the global minimum of each (Ser) (SA) $(W)_n$ (n = 0–3) and (Thr) (SA) $(W)_n$ (n = 0–3) clusters were re-optimized at the level of M06-2X (Zhao and Truhlar, 2007)/6-311++G (3df, 3dp). Frequency calculations were operated for each stationary point to identify the structure is a stable one. Such a computational strategy was reported to give reasonable results for similar clusters (Elm et al., 2012, 2013; Wang et al., 2016). In order to evaluate the reliability of the M06-2X functional used for the current system, the formation Gibbs free energies of clusters (Ser) (SA) and (Tur) (SA) have been calculated by using B3LYP, B3PW91, CAM-B3LYP, M06-2X, PW91PW91 and ωB97X-D methods with 6–311++G (3df, 3pd) basis set. And the result has been compared with that from high-level DLPNO-CCSD(T)/aug-cc-pVTZ calculations by ORCA program (Peterson et al., 2008; Yousaf and Peterson, 2008) (see Table S1 in SI). The mean unsigned deviation (MUD) in Table S1 indicates that CAM-B3LYP, M06-2X and PW91PW91 with 6–311++G (3df, 3pd) basis set match the DLPNO-CCSD(T)/aug-cc-pVTZ single point energy best, with a MUD between 0.52 and 0.82 kcal/mol for the test clusters. Considering that M06-2X method is adopted in previous studies of amino acids clusters, (Elm et al., 2013; Wang et al., 2016) the same functional was chosen to obtain the structures and energetics in this study for a comparison with the previous work.

The thermodynamics of the interaction of sulfuric acid with serine and threonine was evaluated. The interaction energies were calculated by $\Delta G\,(\mathrm{Int}) = G\,(\mathrm{A\_B}) - G(\mathrm{A}) - G(\mathrm{B})$, where $G\,(\mathrm{A\_B})$, $G(\mathrm{A})$ and $G(\mathrm{B})$ are the Gibbs free energy of the cluster, monomer A and monomer B, respectively. The hydrate distribution was also calculated using the Gibbs free energy of stepwise addition of water molecules to form (Ser) (SA) $(W)_n$ (n = 0–3) and (Thr) (SA) $(W)_n$ (n = 0–3) clusters. Such a method was presented in previous studies (Noppel et al., 2002). Based on the obtained global minima of (Ser) (SA) $(W)_n$ (n = 0–3) and (Thr) (SA) $(W)_n$ (n = 0–3) clusters, the optical properties were evaluated. The variations of Rayleigh light scattering intensities, R_n, along with the number of water molecules were calculated at the CAM-B3LYP/aug-cc-pVDZ level of theory, which has been investigated to have a good balance between efficiency and accuracy (Elm et al., 2014; Peng et al., 2015a). The specific formulas for such calculations have been given elsewhere (Elm et al., 2014). The optical properties of (Ser) (SA) $(W)_n$ (n = 0–3) and (Thr) (SA) $(W)_n$ (n = 0–3) clusters were compared with (TMA) (SA) $(W)_n$ (n = 0–3) and (MEA) (SA) $(W)_n$ (n = 0–3) clusters, which are reported to possess high enhancing potential in nucleation (Nadykto et al., 2015; Xie et al., 2017). The (TMA) (SA) $(W)_n$ (n = 0–3) and (MEA) (SA) $(W)_n$ (n = 0–3) clusters were obtained using the same method. The structures of (MEA) (SA) $(W)_n$ (n = 0–3) and (TMA) (SA) $(W)_n$ (n = 0–3) clusters are listed in Fig. S1. The obtained global Gibb free energy minima of (MEA) (SA) $(W)_n$ (n = 0–3) clusters are same as that reported in Xie's study, (Xie et al., 2017) which further validated the reliability of the strategy adopted in this work.

3. Results and discussion

3.1. Structures

In this study, the denotations of Ser_SA_*n*W and Thr_SA_*n*W were used to present the (Ser) (SA) $(W)_n$ (n = 0–3) and (Thr) (SA) $(W)_n$ (n = 0–3) conformations, respectively, where the "*n*" denotes the number of water molecules. The lowest Gibbs free energy structures of each cluster are depicted in Fig. 2. As shown in this figure, the (Thr) (SA) and (Ser) (SA) clusters are featured by a ring structure with two inter-molecular hydrogen bonds, which is similar to the cyclic cluster of (MEA) (SA) (Xie et al., 2017). In these two clusters, the hydroxyl rather than carbonyl group, together with amine group, interacts with SA moiety. It is noted that an intermolecular proton transfer occurred during the interaction. These characteristics differ from the case of (Gly) (SA) and (Ala) (SA) clusters, where interacting groups are amino/acid groups and no proton transfer occurred (Elm et al., 2013; Wang et al., 2016). This indicates that hydroxyl substituent has significant influence on the cluster structures. In addition, unlike (Ser) (SA), (Thr) (SA) shows an additional intra-molecular hydrogen bond (bond length of 1.98 Å, Fig. 2a) in Thr upon complexation with SA, as there is no such hydrogen bond in single Thr molecule (Fig. S2).

With the interaction of water molecules, the structures of (Ser) (SA) $(W)_n$ and (Thr) (SA) $(W)_n$ (n = 1–3) are also different (Fig. 2b). In the former, both hydroxyl and amino groups of Ser are involved in the interaction with water or SA moiety. While in the latter, the interaction manner depends on the number of water molecules. In (Thr) (SA) (W), the carboxyl and hydroxyl groups interact with water and SA moiety. In (Thr) (SA) $(W)_2$ and (Thr) (SA) $(W)_3$, all the three functional groups of Thr are involved in the hydrogen bond interaction. The free group of serine and threonine unparticipated in the hydrogen bonds may be able to involve in the intermolecular interactions in larger clusters, which needs further study to elucidate the interaction modes of amino acids with SA. The structural differences in the hydrated clusters indicate that the methyl substitution of amino acid affects the interaction manner between amino acid and SA. To sum up, these results suggest that different amino acid has different interaction fashion with sulfuric acid and may highlight the needs of study on the effects of various amino acids on aerosol.

It is noteworthy that, in (Thr) (SA) $(W)_2$ and (Thr) (SA) $(W)_3$ clusters, all three functional groups of Thr participate in the intermolecular interactions. Other isomers of (Ser) (SA) $(W)_n$ and (Thr) (SA) $(W)_n$ (n = 1–3) are listed in Fig. S3-S8. As can be seen from these figures, in a certain number of isomers of serine and threonine clusters, all the three functional groups interact with SA and water. It is expected that amino acids with additional non-characteristic functional groups may enhance the interaction with atmospheric nucleation precursors from three directions in certain cases.

3.2. (Thr) (SA) cluster as a potential participant in ion-induced nucleation

Nadykto et al. (Nadykto and Yu, 2008) pointed out that the electrical dipole moment of stable hydrogen-bonded clusters of sulfuric acid is important for ion-induced nucleation, which is largely controlled by dipole-charge interaction of airborne ions with vapor monomers and pre-existing clusters. The immediate vicinity (<1 kcal/mol) of the global minima may be populated with a number of isomers with drastically different dipole moment, leading to strong dipole-ion interaction. The six lowest isomers in energy of (Thr) (SA) and (Ser) (SA) cluster and their corresponding dipole moment are displayed in Fig. 3. The ΔE and ΔG represent the relative electronic energy and the relative Gibbs free energy of cluster to the global minimum at a standard state of 298.15 K and 1 atm. As shown in Fig. 3c, the dipole moments of **Thr_SA_c** and **Thr_SA_f** (8.82 and 9.06 Debye, Table S2) are higher than other isomers including global minimum **Thr_SA_a** (6.08 Debye, Table S2) and isomers of (Ser) (SA) (5.91–8.23 Debye, Table S3). Besides, they are much higher than the reported highest dipole moment of mono-, di-, and trihydrates of the sulfuric acid (3.8, 5.03 and 4.16 Debye, respectively) (Nadykto and Yu, 2008). In addition, the two isomers with highest dipole moments structurally featured by three intermolecular hydrogen bonds between threonine and SA compared with other isomers of (Tur) (SA) (Fig. 3a) and (Ser) (SA)

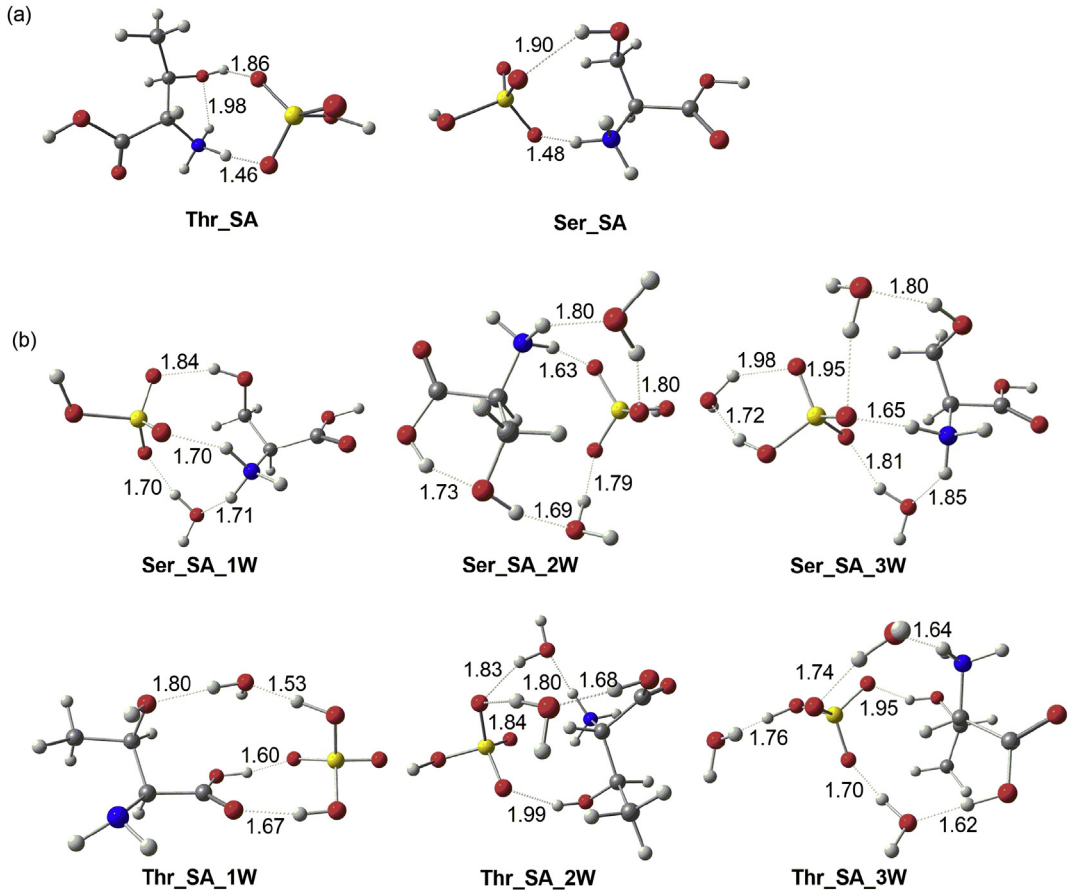

Fig. 2. The lowest Gibbs free energy structures of (Thr) (SA) $(W)_n$ and (Ser) (SA) $(W)_n$ (n = 0–3) at the M06-2X/6-311++G (3df, 3pd) level of theory (oxygen in red, hydrogen in white, sulfur in yellow, carbon in gray and nitrogen in blue). The hydrogen bond lengths are given in Å. (For interpretation of the references to colour in this figure legend, the reader is referred to the Web version of this article.)

(Fig. 3b). Moreover, **Thr_SA_c** may have certain population because of small energy separation (relative free energy of 0.21 kcal/mol) from the global minimum **Thr_SA_a**, which is different from (Ser) (SA) clusters with other isomers being about 1 kcal/mol higher than **Ser_SA_a**. Therefore, **Thr_SA_c** could favorably participate in dipole-ion interaction, which may have important implications for the ion-mediated production of ultrafine aerosol particles associated with various climatic and health impacts (Yu et al., 2012).

3.3. Thermodynamic analysis

The formation Gibbs free energies of the clusters of sulfuric acid with various amino acids, water and SA are summarized in Table 1. By comparing the formation energies of clusters, the relative stabilities of the clusters could be obtained to evaluate their roles in NPF process (Sheng et al., 2017; Zhao et al., 2017). The cluster structures of (SA) (SA) and (SA) $(W)_n$ (n = 1–4) are shown in Fig. S9 and S10 (see SI). The structures of (SA) (SA) and (SA) $(W)_n$ (n = 1–4) are consistent with previous studies (Temelso et al., 2012a, 2012b). The formation electronic energies and enthalpies of these clusters are shown in Table S4.

As shown in Table 1, The calculated formation free energy of −2.5 kcal/mol for the (SA) (W) cluster is in agreement with experimental data (−3.6 ± 1.0 kcal/mol), (Hanson and Eisele, 2000) suggesting the reliability of theoretical method used. It is found that the formations of (Ser) (SA) and (Tur) (SA) clusters are energetically more favorable than that of (SA) (W) and (SA) (SA) clusters (−10.14 and −9.18 kcal/mol *vs.* −2.51 and −8.41 kcal/mol, Table 1). The BSSE-corrected energies listed in Table S5 suggest the same result. This indicates that serine and threonine are capable of stabilizing SA to promote NPF in initial nucleation steps. It is noteworthy that the interaction of (Ser) (SA) is higher than (Thr) (SA) cluster and the previously reported (Gly) (SA) and (Ala) (SA) clusters, which are all calculated at M06-2X/6-311++G (3df, 3pd) level (Table 1). (Elm et al., 2013; Wang et al., 2016) This suggests that serine may play more important role in stabilizing sulfuric acid to promote the initial nucleation steps of NPF compared with threonine, glycine and alanine. As serine and alanine differs in structure by a hydroxyl group, this result indicates that the additional non-characteristic functional group in amino acids may promote their interaction with atmospheric nucleation precursors such as sulfuric acid.

Hydration effect was also evaluated by calculating the formation Gibbs free energies of hydrated (Thr) (SA) and (Ser) (SA) clusters through three formation pathways, as presented in Table 2. The corresponding electronic energies (ΔE) and enthalpies (ΔH) are listed in Tables S6 and S7, respectively. In the total binding path, the ΔG values were calculated by ΔG (Total) = G [(AA) (SA) $(H_2O)_n$] − n G (H_2O) − G (AA) − G (SA). Along with this path, the interaction of monomers within the resulting clusters becomes stronger as the ΔG values become larger with the number of water molecules. In the synthetic binding path, the ΔG values were calculated by ΔG (Synthetic) = G [(AA) (SA) $(H_2O)_n$] − G (AA) − G [(SA) $(H_2O)_n$]. The hydration effects of the first and second water molecules are most obvious, as the ΔG values for the addition of serine and threonine to (SA) (W) and (SA) $(W)_2$ are more favorable than forming (AA) (SA)

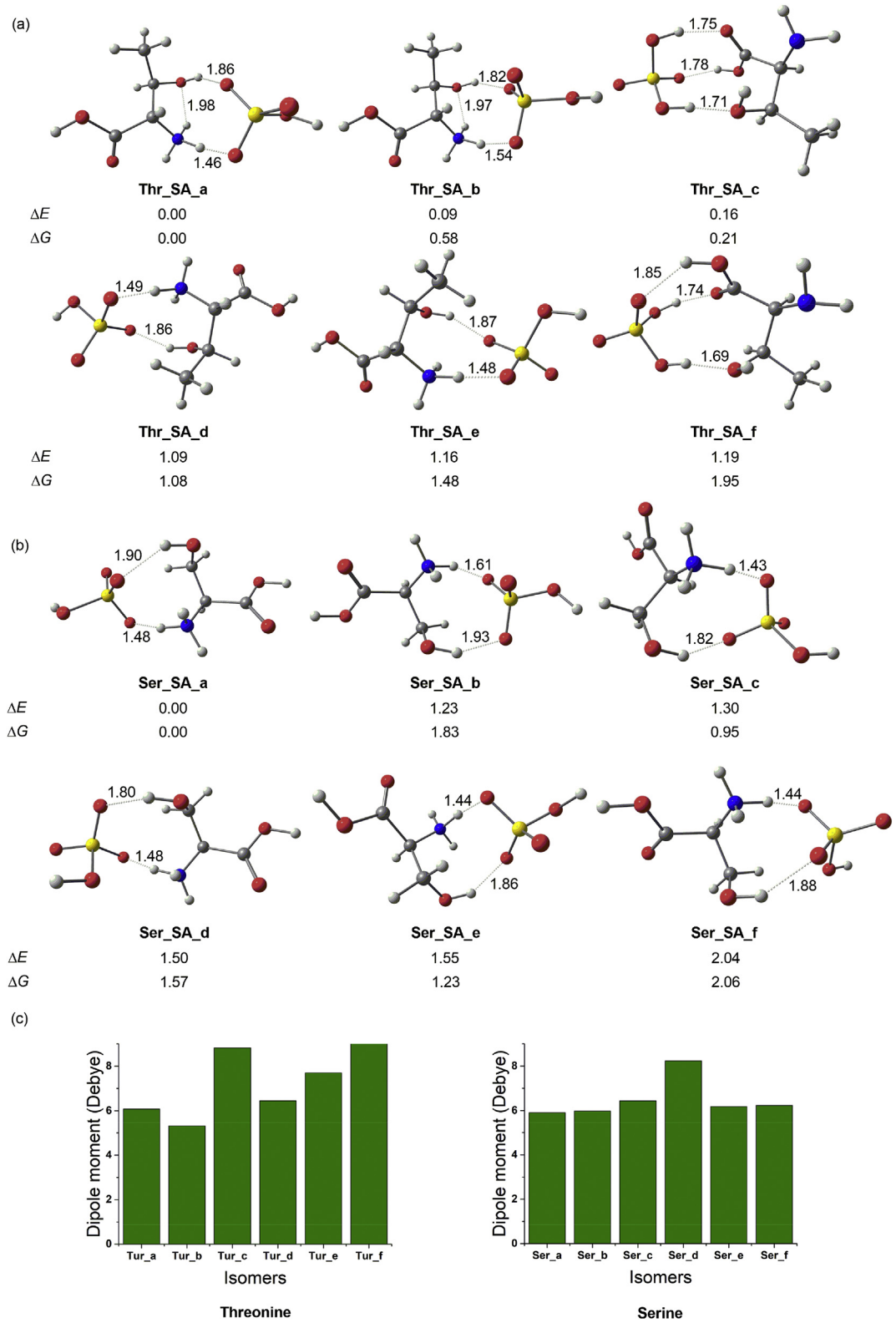

Fig. 3. The optimized geometries and dipole moment of (Thr) (SA) and (Ser) (SA) cluster isomers. (a) Structures of (Thr) (SA) cluster isomers. (b) Structures of (Ser) (SA) cluster isomers at the M06-2X/6-311++G (3df, 3pd) level of theory (oxygen in red, hydrogen in white, sulfur in yellow, carbon in gray and nitrogen in blue). The relative energies are ordered by increasing Δ*E* (given in kcal/mol). The hydrogen bond lengths are given in Å. (c) The dipole moments of isomers of (Thr) (SA) and (Ser) (SA) clusters. (For interpretation of the references to colour in this figure legend, the reader is referred to the Web version of this article.)

Table 1
The formation Gibbs free energies (ΔG, kcal/mol, 298.15 K and 1 atm) of the SA-involved clusters.

Entries	Reactions	ΔG
(1)	Ser + SA → (Ser) (SA)	−10.14
(2)	Tur + SA → (Tur) (SA)	−9.18
(3)	W + SA → (SA) (W)	−2.51
(4)	SA + SA → (SA) (SA)	−8.41
(5)	Gly + SA → (Gly) (SA)	−7.36[a]
(6)	Ala + SA → (Ala) (SA)	−9.41[a]

[a] The results were obtained at the level of M06-2X/6-311++G (3df, 3pd) (see refs. 22,23), which is same as that in this study.

Table 2
The formation Gibbs free energies (kcal/mol) of (Thr) (SA) $(H_2O)_n$ and (Ser) (SA) $(H_2O)_n$ (n = 0–3) clusters through various formation manners.

Amino acid (AA)	AA·SA	AA·SA·H_2O	AA·SA·2H_2O	AA·SA·3H_2O
Total binding path	**AA + SA + nH_2O → (AA) (SA) $(H_2O)_n$**			
Ser	−10.14	−12.93	−15.40	−15.85
Tur	−9.18	−12.89	−15.70	−15.83
Synthetic binding path	**AA + (SA) $(H_2O)_n$ → (AA) (SA) $(H_2O)_n$**			
Ser	−10.14	−10.42	−10.37	−9.01
Tur	−9.18	−10.38	−10.67	−8.99
Stepwise binding path	**(AA) (SA) $(H_2O)_{n-1}$ + H_2O → (AA) (SA) $(H_2O)_n$**			
Ser	−10.14	−2.79	−2.47	−0.45
Tur	−9.18	−3.71	−2.81	−0.13

clusters (−10.42/−10.37 and −10.38/−10.67 kcal/mol *vs.* −10.14 and −9.18 kcal/mol, Table 2). Moreover, an unusual phenomenon was observed in (Thr) (SA) (W), as proton transfer occurs in (Thr) (SA) instead of (Thr) (SA) (W). Thus in this case hydration enhances interaction energy in (Thr) (SA) (W) cluster without promoting proton transfer. In the stepwise binding path, the ΔG values were calculated by ΔG (Stepwise) = G [(AA) (SA) $(H_2O)_n$] − G [(AA) (SA) $(H_2O)_{n-1}$] − G (H_2O). The ΔG values of stepwise binding path are negative, indicating that the formation of hydrated (AA) (SA) clusters is favorable under the conditions applied.

3.4. Hydrate distribution and influence of humidity

The hydrated clusters could be thermodynamically favorably formed, as suggested by the negative formation Gibbs free energy (Table 2). However, the number of water molecules in the clusters is affected by the relative humidity (RH). To access the dominant hydrated clusters in the atmosphere, the hydrate distributions for (Thr) (SA) and (Ser) (SA) clusters were investigated with respect to five values of RH (20%, 40%, 60%, 80%, 100%) under the constant temperature of 298.15 K (Fig. 4). By this means, the relative concentration of each hydrated cluster can be estimated (Temelso et al., 2012a, 2012b).

As shown in Fig. 4a, the sensitivity of the hydrate distributions of (Ser) (SA) $(H_2O)_n$ (n = 0–3) clusters to RH is obvious, especially for the unhydrated and dihydrated clusters. When RH = 20%, the total concentration of the hydrated (Ser) (SA) cluster is mainly dispersed as the unhydrated and monohydrated forms. As RH increases to 40%, the unhydrates, monohydrates and dihydrates disperse averagely with monohydrates being most abundant. When RH is 60%, the relative concentration of unhydrate decreases sharply, while the dominant specie shifts from monohydrate to dihydrate. When RH is above 60%, the percentages of unhydrate and monohydrate decrease while that of dihydrate increases gradually with the increase of RH. The relative percentage of dihydrate reaches almost 60% when RH is 100%. Larger hydrated clusters such as trihydrates are almost nonexistent at various RH.

The distributions of hydrated (Thr) (SA) differ from the (Ser) (SA) case. As shown in Fig. 4b, monohydrates are the most prevalent specie when RH = 20%, followed by dihydrates. The unhydrated clusters comprise a proportion of as much as 15% at a RH of 20%. As RH increases to 40%, the dominant specie shifts from monohydrates to dihydrates. With RH increases from 40% to 100%, the percentage of monohydrates decreases while that of dihydrates increases gradually. The relative percentage of dihydrates reaches almost 75% when RH is 100%. The total concentration of the hydrated (Thr) (SA) clusters is mainly dispersed as the mono- and dihydrates. Similar to hydrated (Ser) (SA) clusters, trihydrated (Thr) (SA) clusters are almost nonexistent at various RH. In conclusion, the hydrate distributions of (Thr) (SA) $(W)_n$ (n = 0–3) and (Ser) (SA) $(W)_n$ (n = 0–3) clusters are more averaged than that of (Ala) (SA) $(W)_n$ (n = 0–3) clusters, where the unhydrated clusters are dominant in most cases (Wang et al., 2016). It can be concluded from Fig. 4 that, unlike alanine clusters, hydrated (Ser) (SA) and (Tur) (SA) clusters could retain water even at low RH, which may due to the hydroxyl group in serine and threonine. Previous studies show that the hydroxyl group in organic compounds could significantly increase the CCN efficiency of organic aerosol (Suda et al., 2014). As nucleated particles can subsequently grow up to the size of CCN, providing up to half of the global CCN budget, (Merikanto et al., 2009) hydrated (Ser) (SA) and (Tur) (SA) clusters pose as an interesting possibility for involvement in CCN formation, affecting the properties and lifetime of clouds.

3.5. Optical properties

Rayleigh scattering is the dominant scattering mechanism of particles with diameters much smaller than the wavelength of the light and contributes largely to the extinction properties, which is one aspect of the direct effect of aerosols (Elm et al., 2015). In this study, the intrinsic Rayleigh light scattering intensities of (Thr) (SA) $(W)_n$ (n = 0–3) and (Ser) (SA) $(W)_n$ (n = 0–3) clusters were investigated (Fig. 5). The (MEA) (SA) $(W)_n$ (n = 0–3) and (TMA) (SA) $(W)_n$ (n = 0–3) clusters were also studied for a comparison.

As shown in Fig. 5, the Rayleigh light scattering intensities of unhydrated (Ser) (SA) and (Thr) (SA) clusters are around 450000 a.u. and 550000 a.u., respectively. These values gradually increased to 750000 a.u. for (Ser) (SA) $(W)_3$ and 850000 a.u. for (Thr) (SA) $(W)_3$ with addition of water molecules. This result is consistent with previous study that the Rayleigh light scattering intensity depends on the number of water molecules involved in the cluster (Elm et al., 2014). Moreover, the Rayleigh light scattering intensities for (Thr) (SA) $(W)_n$ (n = 0–3) and (Ser) (SA) $(W)_n$ (n = 0–3) are higher than (MEA) (SA) $(W)_n$ (n = 0–3) (300000–550000 a.u.), (TMA) (SA) $(W)_n$ (n = 0–3) (350000–600000 a.u.) and oxalic acid-containing clusters such as $(H_2C_2O_4)$ (NH_3) $(H_2O)_n$ (n = 1–3) (150000–350000 a.u.), (Peng et al., 2016) $(H_2C_2O_4)$ $(NH_3)_2(H_2O)_n$ (n = 1–3) (200000–450000 a.u.), (Peng et al., 2016) $(H_2C_2O_4)$ $(NH_3)_n$ (n = 1–6) (150000–750000 a.u.) (Peng et al., 2015b) and $(H_2C_2O_4)$ (H_2SO_4) $(H_2O)_n$ (n = 0–5) (300000–700000 a.u.) (Miao et al., 2015) reported in previous studies calculated at the same level CAM-B3LYP/aug-cc-pVTZ by using the same formula. These results indicate that the amino acids such as serine and threonine-containing pre-nucleation clusters scatter light more efficiently than the TMA, MEA and $H_2C_2O_4$-involved counterparts, and thus have greater contribution to the extinction properties of aerosol. As discussed above, the (Thr) (SA) and (Ser) (SA) clusters may retain water molecule at low RH. The higher Rayleigh light scattering intensity of (Thr) (SA) and (Ser) (SA) clusters and the further promotion by addition of water molecules indicate the large light scattering coefficients of aerosol formed via participation of serine and threonine at low RH, which needs to be further validated by

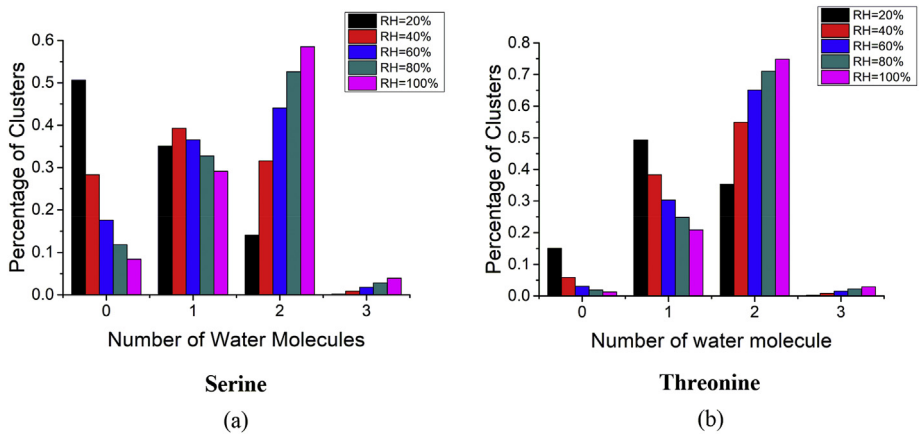

Fig. 4. Hydrate distributions of (a) (Ser) (SA) $(W)_n$ (n = 0–3) and (b) (Thr) (SA) $(W)_n$ (n = 0–3) clusters at five different relative humidities under 298.15 K.

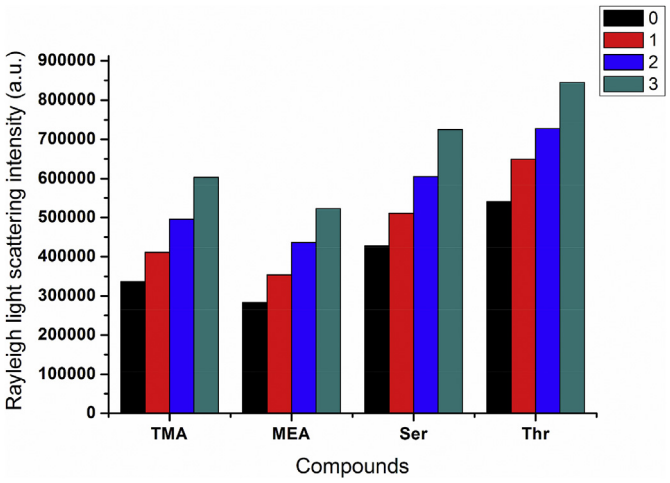

Fig. 5. Intrinsic Rayleigh light scattering intensities of trimethylamine, monoethanolamine, serine and threonine clusters with sulfuric acid as a function of the number of water molecules (n = 0–3).

experiments.

Meanwhile, (Thr) (SA) $(W)_n$ (n = 0–3) possess higher Rayleigh light scattering intensities than (Ser) (SA) $(W)_n$ (n = 0–3), indicating that a methyl substitution could increase the Rayleigh light scattering intensity. This is consistent with the result that the Rayleigh light scattering intensities of (Me_3N) (SA) $(W)_n$ (n = 0–3) can reach to 600000 a.u. while the highest value for $(MeNH_2)$ (SA) $(W)_n$ (n = 0–3) is about 350000 a.u (Lv et al., 2015). This suggests that the compounds with more methyl substitutions are worthy of considering when evaluating the extinction properties of aerosols. In addition, the Rayleigh light intensity of (Ser) (SA) $(W)_n$ is much larger than that of (MEA) (SA) $(W)_n$ (n = 0–3) (Fig. 5), which differs in structure by an additional carboxyl group in serine, indicating that carboxyl group of organics may also enhance the Rayleigh light scattering intensity of clusters.

Although the pure DFT method has been utilized to optimize the cluster structures in this study, the integrated two-layer method such as quantum/molecular mechanics (QM/MM) may be used, in the near future, for constructing larger clusters to obtain more knowledge about amino acids participated in nucleation in atmosphere, which was successfully applied for theoretical treatments of environment-related reactions (Li et al., 2016; Kumar et al., 2018).

4. Conclusions

In this work, quantum chemical calculations have been performed to investigate the geometries, formation Gibbs free energies, hydrate distributions, and Rayleigh light scattering intensities of (Thr) (SA) $(W)_n$ and (Ser) (SA) $(W)_n$ (n = 0–3) clusters. Results show that, in (Thr) (SA) and (Ser) (SA) clusters, serine and threonine form a cyclic structure with SA by both hydroxyl and amino groups. A proton transfer event could occur without participation of water. Geometries of (Thr) (SA) $(W)_n$ and (Ser) (SA) $(W)_n$ (n = 0–3) are also different. These differences indicate that hydroxyl group and different methyl substitution affect the structure of clusters. Besides, threonine can interact with H_2SO_4 and H_2O in three directions in (Thr) (SA) $(W)_2$ and (Thr) (SA) $(W)_3$. Moreover, threonine may serve as a potential participant in ion-induced nucleation due to the high dipole moment of (Thr) (SA) cluster. From thermodynamic analysis, the interaction of serine with sulfuric acid is strongest compared with threonine, glycine and alanine, indicating that serine may play more important role in stabilizing sulfuric acid to promote the initial nucleation steps of new particle formation. In addition, the hydration effects of the first and second water molecules are most obvious. Particularly, in (Thr) (SA) (W), hydration enhances interaction between threonine and sulfuric acid without proton transfer. The hydrate distributions analysis indicated that hydrated (Ser) (SA) and (Tur) (SA) clusters could retain water even at low RH, which may due to the hydroxyl group in serine and threonine. The Rayleigh light scattering intensities of (Thr) (SA) $(W)_n$ and (Ser) (SA) $(W)_n$ (n = 0–3) are much higher than trimethylamine, monoethanolamine and oxalic acid-involved counterparts, indicating the greater influence of amino acid participated pre-nucleation clusters on the extinction properties of aerosols. Besides, carboxyl group and methyl substitution in organics could enhance the Rayleigh light scattering intensity of related clusters. This study may bring new insight into the role of amino acids in initial steps of new particle formation from molecular level and could help better understand the properties of amino acid-containing organic aerosol.

Associated content

Electronic Supplementary Information (ESI) available: it contains additional tables and figures accompanying the manuscript and the optimized coordinates of the stationary points.

Acknowledgements

This work was supported by the National Key Research and Development Program of China (2016YFC0202200) and the Fundamental Research Funds for the Central Universities (DUT18GJ201, DUT18RC(3)002). The authors also thank the Network and Information Center of the Dalian University of Technology for part of computational resources.

Appendix A. Supplementary data

Supplementary data related to this article can be found at https://doi.org/10.1016/j.chemosphere.2018.07.014.

References

Arquero, K.D., Xu, J., Gerber, R.B., Finlayson-Pitts, B.J., 2017. particle formation and growth from oxalic acid, methanesulfonic acid, trimethylamine and water: a combined experimental and theoretical study. Phys. Chem. Chem. Phys. 19 (41), 28286–28301.

Arquero, K.D., Gerber, R.B., Finlayson-Pitts, B.J., 2017. The role of oxalic acid in new particle formation from methanesulfonic acid, methylamine, and water. Environ. Sci. Technol. 51 (4), 2124–2130.

Baker, M.B., Peter, T., 2008. Small-scale cloud processes and climate. Nature 451 (7176), 299–300.

Barbaro, E., Zangrando, R., Moret, I., Barbante, C., Cescon, P., Gambaro, A., 2011. Free amino acids in atmospheric particulate matter of venice, Italy. Atmos. Environ. 45 (28), 5050–5057.

Barbaro, E., Zangrando, R., Padoan, S., Karroca, O., Toscano, G., Cairns, W.R.L., Barbante, C., Gambaro, A., 2017. Aerosol and snow transfer processes: an investigation on the behavior of water-soluble organic compounds and ionic species. Chemosphere 183, 132–138.

Choi, J.-K., Ban, S.-J., Kim, Y.-P., Kim, Y.-H., Yi, S.-M., Zoh, K.-D., 2015. Molecular marker characterization and source appointment of particulate matter and its organic aerosols. Chemosphere 134, 482–491.

Dimitriou, K., Kassomenos, P., 2017. Airborne heavy metals in two cities of north rhine westphalia–performing inhalation cancer risk assessment in terms of atmospheric circulation. Chemosphere 186, 78–87.

Elm, J., Bilde, M., Mikkelsen, K.V., 2012. Assessment of density functional theory in predicting structures and free energies of reaction of atmospheric prenucleation clusters. J. Chem. Theor. Comput. 8 (6), 2071–2077.

Elm, J., Fard, M., Bilde, M., Mikkelsen, K.V., 2013. Interaction of Glycine with common atmospheric nucleation precursors. J. Phys. Chem. 117 (48), 12990–12997.

Elm, J., Norman, P., Bilde, M., Mikkelsen, K.V., 2014. Computational study of the Rayleigh light scattering properties of atmospheric pre-nucleation clusters. Phys. Chem. Chem. Phys. 16 (22), 10883–10890.

Elm, J., Norman, P., Mikkelsen, K.V., 2015. Rayleigh light scattering properties of atmospheric molecular clusters consisting of sulfuric acid and bases. Phys. Chem. Chem. Phys. 17 (24), 15701–15709.

Elm, J., Myllys, N., Kurten, T., 2017. What is required for highly oxidized molecules to form clusters with sulfuric acid? J. Phys. Chem. 121 (23), 4578–4587.

Frisch, M.J., et al., 2016. Gaussian 09, Revision A.02. Gaussian, Inc, Wallingford CT.

Ge, X., Wexler, A.S., Clegg, S.L., 2011. Atmospheric amines – Part I. A review. Atmos. Environ. 45 (3), 524–546.

Hanson, D.R., Eisele, F., 2000. Diffusion of H_2SO_4 in humidified Nitrogen: hydrated H_2SO_4. J. Phys. Chem. 104 (8), 1715–1719.

Kulmala, M., Lehtinen, K.E.J., Laaksonen, A., 2006. Cluster activation theory as an explanation of the linear dependence between formation rate of 3nm particles and sulphuric acid concentration. Atmos. Chem. Phys. 6, 787–793.

Kumar, M., Zhong, J., Zeng, X.C., Francisco, J.S., 2018. Reaction of criegee intermediate with nitric acid at the air-water interface. J. Am. Chem. Soc. 140 (14), 4913–4921.

Leach, J., Blanch, A., Bianchi, A.C., 1999. Volatile organic compounds in an urban airborne environment adjacent to a municipal incinerator, waste collection centre and sewage treatment plant. Atmos. Environ. 33 (26), 4309–4325.

Li, Y., Zhang, R., Du, L., Zhang, Q., Wang, W., 2016. Catalytic mechanism of C–F bond cleavage: insights from QM/MM analysis of fluoroacetate dehalogenase. Catal. Sci. Technol. 6 (1), 73–80.

Li, H., Kupiainen-Määttä, O., Zhang, H., Zhang, X., Ge, M., 2017. A molecular-scale study on the role of lactic acid in new particle formation: influence of relative humidity and temperature. Atmos. Environ. 166, 479–487.

Lin, X.-X., Liu, Y.-R., Huang, T., Xu, K.-M., Zhang, Y., Jiang, S., Gai, Y.-B., Zhang, W.-J., Huang, W., 2014. Theoretical studies of the hydration reactions of stabilized criegee intermediates from the ozonolysis of β-pinene. RSC Adv. 4 (54), 28490–28498.

Luo, Y., Maeda, S., Ohno, K., 2007. Quantum chemistry study of $H^+(H_2O)_8$: a global search for its isomers by the scaled hypersphere search method, and its thermal behavior. J. Phys. Chem. 111 (42), 10732–10737.

Lv, S.-S., Miao, S.-K., Ma, Y., Zhang, M.-M., Wen, Y., Wang, C.-Y., Zhu, Y.-P., Huang, W., 2015. Properties and atmospheric implication of methylamine–sulfuric acid–water clusters. J. Phys. Chem. 119 (32), 8657–8666.

Lyu, X.P., Guo, H., Cheng, H.R., Wang, D.W., 2018. New particle formation and growth at a suburban site and a background site in Hong Kong. Chemosphere 193, 664–674.

Maeda, S., Ohno, K., 2005. Global mapping of equilibrium and transition structures on potential energy surfaces by the scaled hypersphere search Method: applications to ab initio surfaces of formaldehyde and propyne molecules. J. Phys. Chem. 109 (25), 5742–5753.

Maeda, S., Ohno, K., 2007. Structures of water octamers $(H_2O)_8$: exploration on ab initio potential energy surfaces by the scaled hypersphere search method. J. Phys. Chem. 111 (20), 4527–4534.

Maeda, S., Ohno, K., 2008. Microsolvation of hydrogen Sulfide: exploration of $H_2S{\cdot}(H_2O)_n$ and $SH^-{\cdot}H3O^+{\cdot}(H_2O)_{n-1}$ ($n = 5–7$) cluster structures on ab initio potential energy surfaces by the scaled hypersphere search method. J. Phys. Chem. 112 (13), 2962–2968.

Matos, J.T.V., Duarte, R.M.B.O., Duarte, A.C., 2016. Challenges in the identification and characterization of free amino acids and proteinaceous compounds in atmospheric aerosols: a critical review. Trac. Trends Anal. Chem. 75, 97–107.

Merikanto, J., Spracklen, D.V., Mann, G.W., Pickering, S.J., Carslaw, K.S., 2009. Impact of nucleation on global CCN. Atmos. Chem. Phys. 9 (21), 8601–8616.

Metzger, A., Verheggen, B., Dommen, J., Duplissy, J., Prevot, A.S., Weingartner, E., Riipinen, I., Kulmala, M., Spracklen, D.V., Carslaw, K.S., Baltensperger, U., 2010. Evidence for the role of organics in aerosol particle formation under atmospheric conditions. Proc. Natl. Acad. Sci. U. S. A. 107 (15), 6646–6651.

Miao, S.-K., Jiang, S., Chen, J., Ma, Y., Zhu, Y.-P., Wen, Y., Zhang, M.-M., Huang, W., 2015. Hydration of a sulfuric acid-oxalic acid complex: acid dissociation and its atmospheric implication. RSC Adv. 5 (60), 48638–48646.

Nadykto, A.B., Yu, F., 2008. Anomalously large difference in dipole moment of isomers with nearly identical thermodynamic stability. J. Phys. Chem. 112 (31), 7222–7226.

Nadykto, A., Herb, J., Yu, F., Xu, Y., Nazarenko, E., 2015. Estimating the lower limit of the impact of amines on nucleation in the Earth's atmosphere. Entropy 17 (5), 2764–2780.

Noppel, M., Vehkamäki, H., Kulmala, M., 2002. An improved model for hydrate formation in sulfuric acid–water nucleation. J. Chem. Phys. 116 (1), 218–228.

Ohno, K., Maeda, S., 2004. A scaled hypersphere search method for the topography of reaction pathways on the potential energy surface. Chem. Phys. Lett. 384 (4–6), 277–282.

Ohno, K., Maeda, S., 2006. Global reaction route mapping on potential energy surfaces of formaldehyde, formic acid, and their metal-substituted analogues. J. Phys. Chem. 110 (28), 8933–8941.

Omori, K., Nakayama, H., Ishii, K., 2014. Diversity of the dimer structures of toluene: exploration by the GRRM method. Chem. Lett. 43 (11), 1803–1805.

Paula, A.S., Matos, J.T.V., Duarte, R.M.B.O., Duarte, A.C., 2016. Two chemically distinct light-absorbing pools of urban organic aerosols: a comprehensive multidimensional analysis of trends. Chemosphere 145, 215–223.

Peng, X.-Q., Liu, Y.-R., Huang, T., Jiang, S., Huang, W., 2015. Interaction of gas phase oxalic acid with ammonia and its atmospheric implications. Phys. Chem. Chem. Phys. 17 (14), 9552–9563.

Peng, X.-Q., Liu, Y.-R., Huang, T., Jiang, S., Huang, W., 2015. Interaction of gas phase oxalic acid with ammonia and its atmospheric implications. Phys. Chem. Chem. Phys. 17 (14), 9552–9563.

Peng, X.-Q., Huang, T., Miao, S.-K., Chen, J., Wen, H., Feng, Y.-J., Hong, Y., Wang, C.-Y., Huang, W., 2016. Hydration of oxalic acid-ammonia complex: atmospheric implication and Rayleigh-Scattering properties. RSC Adv. 6 (52), 46582–46593.

Peterson, K.A., Adler, T.B., Werner, H.J., 2008. Systematically convergent basis sets for explicitly correlated wavefunctions: the atoms H, He, B–Ne, and Al–Ar. J. Chem. Phys. 128 (8), 084102–084112.

Rothfuss, N.E., Petters, M.D., 2016. Influence of functional groups on the viscosity of organic aerosol. Environ. Sci. Technol. 51 (1), 271–279.

Saikia, J., Narzary, B., Roy, S., Bordoloi, M., Saikia, P., Saikia, B.K., 2016. Nanominerals, fullerene aggregates, and hazardous elements in coal and coal combustion-generated aerosols: an environmental and toxicological assessment. Chemosphere 164, 84–91.

Scalabrin, E., Zangrando, R., Barbaro, E., Kehrwald, N.M., Gabrieli, J., Barbante, C., Gambaro, A., 2012. Amino acids in arctic aerosols. Atmos. Chem. Phys. 12 (21), 10453–10463.

Sheng, X., Zhao, H., Du, L., 2017. Molecular understanding of the interaction of methyl hydrogen sulfate with ammonia/dimethylamine/water. Chemosphere 186, 331–340.

Shi, X., Zhang, R., Sun, Y., Xu, F., Zhang, Q., Wang, W., 2018. A density functional theory study of aldehydes and their atmospheric products participating in nucleation. Phys. Chem. Chem. Phys. 20 (2), 1005–1011.

Suda, S.R., Petters, M.D., Yeh, G.K., Strollo, C., Matsunaga, A., Faulhaber, A., Ziemann, P.J., Prenni, A.J., Carrico, C.M., Sullivan, R.C., Kreidenweis, S.M., 2014. Influence of functional groups on organic aerosol cloud condensation nucleus activity. Environ. Sci. Technol. 48 (17), 10182–10190.

Temelso, B., Morrell, T.E., Shields, R.M., Allodi, M.A., Wood, E.K., Kirschner, K.N., Castonguay, T.C., Archer, K.A., Shields, G.C., 2012. Quantum mechanical study of sulfuric acid hydration: atmospheric implications. J. Phys. Chem. 116 (9), 2209–2224.

Temelso, B., Phan, T.N., Shields, G.C., 2012. Computational study of the hydration of sulfuric acid dimers: implications for acid dissociation and aerosol formation. J. Phys. Chem. 116 (39), 9745–9758.

Wang, C.-Y., Ma, Y., Chen, J., Jiang, S., Liu, Y.-R., Wen, H., Feng, Y.-J., Hong, Y.,

Huang, T., Huang, W., 2016. Bidirectional interaction of alanine with sulfuric acid in the presence of water and the atmospheric implication. J. Phys. Chem. 120 (15), 2357–2371.
Xie, H.-B., Elm, J., Halonen, R., Myllys, N., Kurtén, T., Kulmala, M., Vehkamäki, H., 2017. Atmospheric fate of monoethanolamine: enhancing new particle formation of sulfuric acid as an important removal process. Environ. Sci. Technol. 51 (15), 8422–8431.
Yousaf, K.E., Peterson, K.A., 2008. Optimized auxiliary basis sets for explicitly correlated methods. J. Chem. Phys. 129 (18), 184108.
Yu, F., Luo, G., Liu, X., Easter, R.C., Ma, X., Ghan, S.J., 2012. Indirect radiative forcing by ion-mediated nucleation of aerosol. Atmos. Chem. Phys. 12 (23), 11451–11463.
Zhang, Q., Anastasio, C., 2003. Free and combined amino compounds in atmospheric fine particles (PM2.5) and fog waters from northern California. Atmos. Environ. 37 (16), 2247–2258.
Zhang, Q., Anastasio, C., Jimenez-Cruz, M., 2002. Water-soluble organic nitrogen in atmospheric fine particles (PM2.5) from northern California. J. Geophys. Res.: Atmos. 107 (D11). AAC 3-1-AAC 3–9.
Zhang, R., Suh, I., Zhao, J., Zhang, D., Fortner, E.C., Tie, X., Molina, L.T., Molina, M.J., 2004. Atmospheric new particle formation enhanced by organic acids. Science 304 (5676), 1487.
Zhang, R., Khalizov, A., Wang, L., Hu, M., Xu, W., 2011. Nucleation and growth of nanoparticles in the atmosphere. Chem. Rev. 112 (3), 1957–2011.
Zhao, Y., Truhlar, D.G., 2007. The M06 suite of density functionals for main group thermochemistry, thermochemical kinetics, noncovalent interactions, excited states, and transition elements: two new functionals and systematic testing of four m06-class functionals and 12 other functionals. Theor. Chem. Acc. 120 (1–3), 215–241.
Zhao, H., Jiang, X., Du, L., 2017. Contribution of methane sulfonic acid to new particle formation in the atmosphere. Chemosphere 174, 689–699.